



# Throughflow effect on bi-disperse convection

Florinda Capone<sup>1</sup> · Roberta De Luca<sup>1</sup> · Giuliana Massa<sup>1</sup>

Received: 22 June 2023 / Accepted: 11 August 2023 / Published online: 28 August 2023  
© The Author(s) 2023

## Abstract

The aim of this paper is to investigate the effect of a vertical constant throughflow on convective instabilities in a horizontal layer of fluid-saturated bi-disperse porous medium heated from below. Via linear instability and nonlinear stability analyses of the throughflow solution, the linear and nonlinear critical Rayleigh numbers for convective instabilities have been determined and studied as functions of the strength of the throughflow.

**Keywords** Bi-disperse porous media · Throughflow · Instability analysis · Nonlinear stability

**Mathematics Subject Classification** 76E06 · 76Exx · 76S05 · 76Sxx

## 1 Introduction

Bi-disperse convection is the analysis of the onset of convection in dual porosity materials, called bi-disperse porous media. A bi-disperse porous medium (BDPM) is a material characterized by two types of pores called macropores—with porosity

---

Florinda Capone, Roberta De Luca and Giuliana Massa have equally contributed to this work.

---

This paper is in memory of Prof. Salvatore Rionero. F. Capone and R. De Luca dedicate this paper to their beloved Mentor Prof. Rionero, remembering him both for his human and scientific qualities and thanking him for all his teachings they will never forget. “Rare are those people who use the mind, few use the heart and really unique are those who use both” (R. Levi-Montalcini).

---

✉ Florinda Capone  
fcapone@unina.it

Roberta De Luca  
roberta.deluca@unina.it

Giuliana Massa  
giuliana.massa@unina.it

<sup>1</sup> Dipartimento di Matematica e Applicazioni ‘R.Caccioppoli’, Università degli Studi di Napoli Federico II, Via Cintia, Monte S. Angelo, Naples 80126, Italy

$\phi$ —and micropores—with porosity  $\epsilon$ . Therefore,  $(1 - \phi)\epsilon$  is the fraction of volume occupied by the micropores,  $\phi + (1 - \phi)\epsilon$  is the fraction of volume occupied by the fluid,  $(1 - \epsilon)(1 - \phi)$  is the fraction of volume occupied by the solid skeleton. In particular, the macropores are referred to as f-phase (fractured phase), while the remainder of the structure is referred to as p-phase (porous phase). The first refined mathematical model describing the onset of bi-disperse convection was proposed by Nield and Kuznetsov in [1–3], where the authors analysed the onset of convection in a horizontal layer of BDPM saturated by a non-isothermal incompressible fluid heated from below, proposing a model with two seepage velocities  $\mathbf{v}^f$  and  $\mathbf{v}^p$ , two pressures  $p^f$  and  $p^p$  and two temperature fields  $T^f$  and  $T^p$ . Nield and Kuznetsov proved that the critical Rayleigh number for the onset of bi-disperse convection is higher with respect to the critical Rayleigh number for the single porosity case, therefore dual porosity materials are better suited for insulation problems and thermal management problems. Hence, bi-disperse porous materials offer much more possibilities to design man-made materials for heat transfer problems and for this reason the onset of bi-disperse convection has recently attracted the attention of many researchers [4–6]. In this paper, we will focus the attention on single-temperature bi-disperse porous media (i.e.  $T^f = T^p$ ), since a single-temperature model may suffice to represent many real situations and the resulting mathematical model is consistent with experiments related to heat transfer and thermal dispersion in bi-disperse porous media [7, 8].

The relevance of the analysis of non-isothermal steady flow of fluids through porous materials called throughflow is due to the effect that such flow has on convective instabilities. When a vertical net mass flow (throughflow) is present across a horizontal layer heated from below, the problem to determine until this motion is stable is of fundamental importance, due to the possibility of controlling the convective instabilities by adjusting the strength of the throughflow, especially in applications involving cloud physics, hydrological/geophysical studies, seabed hydrodynamics, subterranean pollution, and many industrial and technological processes [9–11]. Keeping in mind these applications, the use of dual porosity materials for thermal management problems and the relevance of regulating convective instabilities for thermal and engineering sciences, in this paper the onset of convective instability in a fluid-saturated bi-disperse porous layer heated from below is analysed, assuming that there is a vertical net mass flow across the layer. The paper is organized as follows. In Sect. 2 the mathematical model is presented, along with the equations governing the evolutionary behaviour of the perturbation to the throughflow solution. In Sect. 3 the linear instability analysis of the throughflow solution is performed, in order to find the instability threshold for the onset of convective instabilities and the effect of the vertical constant throughflow on the instability threshold is numerically analysed. In Sect. 4, the nonlinear stability analysis of the throughflow solution is performed via the differential constraints approach and the weighted energy method in order to catch the method that better describes the physics of the problem. Via numerical simulations, the stability thresholds are compared to the instability ones and analysed as functions of the Peclet number. Section 5 is a concluding section that recaps the obtained results.

## 2 Mathematical model

Introducing a reference frame  $Oxyz$  with fundamental unit vectors  $\mathbf{i}, \mathbf{j}, \mathbf{k}$  ( $\mathbf{k}$  pointing vertically upward), let us consider a plane layer  $L = \mathbb{R}^2 \times [0, d]$  of bi-disperse porous medium saturated by a non-isothermal fluid and uniformly heated from below. Let us employ a single temperature bi-disperse porous medium, i.e.  $T^f = T^p = T$ . An Oberbeck-Boussinesq approximation is assumed: the fluid density  $\rho$  is constant in all terms of the governing equations, except in the body force term (due to the gravity  $\mathbf{g} = -g\mathbf{k}$ ), where we choose a linear dependence on temperature, i.e.  $\rho = \rho_0[1 - \alpha(T - T_0)]$ ,  $\alpha$  being the thermal expansion coefficient and  $\rho_0$  being the constant fluid density at the reference temperature  $T_0$ . Let us underline that this assumption is experimentally and thermodynamically consistent if  $p \ll p_{CR} = \frac{c_p \rho_0}{\alpha}$ ,  $p$  being the pressure field, while  $c_p$  is the specific heat at constant pressure. In particular, in [12] the authors proved that if  $p \ll p_{CR}$ , the Oberbeck-Boussinesq approximation is compatible with the entropy principle. Therefore, the governing equations, according to the Darcy's model, are, cf. [8],

$$\begin{cases} -\frac{\mu}{K_f} \mathbf{v}^f - \zeta(\mathbf{v}^f - \mathbf{v}^p) - \nabla p^f + \rho_0 \alpha g T \mathbf{k} = \mathbf{0}, \\ -\frac{\mu}{K_p} \mathbf{v}^p - \zeta(\mathbf{v}^p - \mathbf{v}^f) - \nabla p^p + \rho_0 \alpha g T \mathbf{k} = \mathbf{0}, \\ \nabla \cdot \mathbf{v}^f = 0, \\ \nabla \cdot \mathbf{v}^p = 0, \\ (\rho c)_m \frac{\partial T}{\partial t} + (\rho c)_f (\mathbf{v}^f + \mathbf{v}^p) \cdot \nabla T = k_m \Delta T, \end{cases} \tag{1}$$

where  $\mathbf{x} = (x, y, z)$ ,  $T$  is the temperature field,  $p^s$  and  $\mathbf{v}^s$  are pressure field and seepage velocity for  $s = \{f, p\}$ , respectively,  $\zeta$  is the interaction coefficient between the f-phase and the p-phase,  $\mu$  is the fluid viscosity,  $K_s$  are the permeabilities for  $s = \{f, p\}$ ,  $k_m$  is the thermal conductivity, respectively. Moreover,  $(\rho c)_m = (1 - \phi)(1 - \epsilon)(\rho c)_{sol} + \phi(\rho c)_f + \epsilon(1 - \phi)(\rho c)_p$ ,  $k_m = (1 - \phi)(1 - \epsilon)k_{sol} + \phi k_f + \epsilon(1 - \phi)k_p$  (the subscript *sol* is referred to the solid skeleton). Since we are confining ourselves in the case of a single temperature BDPM and macropores and micropores are saturated by the same fluid, we expect  $(\rho c)_f$  and  $(\rho c)_p$  to be the same, hence  $(\rho c)_m = (1 - \phi)(1 - \epsilon)(\rho c)_{sol} + [\phi + \epsilon(1 - \phi)](\rho c)_f$ , see [13].

We are interested in the stability analysis of a vertical throughflow present across the layer  $L$ , therefore to (1) we append the following boundary conditions

$$\mathbf{v}^s = Q^s \mathbf{k}, \text{ on } z=0, d \text{ for } s = \{f, p\}, \quad T = T_L \text{ on } z=0, \quad T = T_U \text{ on } z=d \tag{2}$$

where  $T_L > T_U$ , since the layer is heated from below, and  $Q^s$  are constants ( $s = \{f, p\}$ ).

The steady constant non-isothermal fluid flow solution to (1)–(2) called *throughflow*

is given by

$$\bar{\mathbf{v}}^f = Q^f \mathbf{k}, \quad \bar{\mathbf{v}}^p = Q^p \mathbf{k}, \quad \bar{T} = \frac{T_U - T_L e^{\bar{Q}d/k} + (T_L - T_U) e^{\bar{Q}z/k}}{1 - e^{\bar{Q}d/k}} \tag{3}$$

where  $\bar{Q} = Q^f + Q^p$ , while  $k = \frac{k_m}{(\rho c)_f}$  is the thermal diffusivity. Let us introduce a generic perturbation  $\{\mathbf{u}^f, \mathbf{u}^p, \theta, \gamma, \pi^f, \pi^p\}$  to the throughflow solution, with  $\mathbf{u}^f = (u^f, v^f, w^f)$  and  $\mathbf{u}^p = (u^p, v^p, w^p)$ . The equations describing the behaviour of the perturbations fields are

$$\begin{cases} -\frac{\mu}{K_f} \mathbf{u}^f - \zeta(\mathbf{u}^f - \mathbf{u}^p) - \nabla \pi^f + \rho_0 \alpha g \theta \mathbf{k} = \mathbf{0}, \\ -\frac{\mu}{K_p} \mathbf{u}^p - \zeta(\mathbf{u}^p - \mathbf{u}^f) - \nabla \pi^p + \rho_0 \alpha g \theta \mathbf{k} = \mathbf{0}, \\ \nabla \cdot \mathbf{u}^f = 0, \\ \nabla \cdot \mathbf{u}^p = 0, \\ (\rho c)_m \frac{\partial \theta}{\partial t} + (\rho c)_f (\mathbf{u}^f + \mathbf{u}^p) \cdot \nabla \theta = -(\rho c)_f (w^f + w^p) \frac{\partial \bar{T}}{\partial z} - (\rho c)_f \bar{Q} \frac{\partial \theta}{\partial z} + k_m \Delta \theta, \end{cases} \tag{4}$$

under the boundary conditions

$$w^f = w^p = \theta = 0, \quad \text{on } z = 0, d. \tag{5}$$

To derive the dimensionless perturbation equations, we introduce the following non-dimensional parameters:

$$\mathbf{x}^* = \frac{\mathbf{x}}{d}, \quad t^* = \frac{t}{t^\#}, \quad \theta^* = \frac{\theta}{T^\#}, \quad \gamma_1 = \frac{\mu}{K_f \zeta}, \quad \gamma_2 = \frac{\mu}{K_p \zeta}, \quad \mathbf{u}^{s*} = \frac{\mathbf{u}^s}{U}, \quad \pi^{s*} = \frac{\pi^s}{p^\#}, \quad \text{for } s = \{f, p\}$$

with the following scales

$$U = \frac{\zeta k_m}{(\rho c)_f d}, \quad t^\# = \frac{d^2 (\rho c)_m}{k_m}, \quad p^\# = \frac{k_m \zeta}{(\rho c)_f}, \quad T^\# = \sqrt{\frac{\beta k_m \zeta}{(\rho c)_f \rho_0 \alpha g}},$$

and define the Darcy-Rayleigh number  $\mathcal{R}$  and the Peclet number  $Pe$  as

$$\mathcal{R} = \sqrt{\frac{\beta d^2 (\rho c)_f \rho_0 \alpha g}{\zeta k_m}}, \quad Pe = \frac{\bar{Q} d}{k}.$$

The dimensionless equations governing the perturbation fields, dropping the asterisks, are

$$\begin{cases} -\gamma_1 \mathbf{u}^f - (\mathbf{u}^f - \mathbf{u}^p) - \nabla \pi^f + \mathcal{R} \theta \mathbf{k} = \mathbf{0}, \\ -\gamma_2 \mathbf{u}^p - (\mathbf{u}^p - \mathbf{u}^f) - \nabla \pi^p + \mathcal{R} \theta \mathbf{k} = \mathbf{0}, \\ \nabla \cdot \mathbf{u}^f = 0, \\ \nabla \cdot \mathbf{u}^p = 0, \\ \frac{\partial \theta}{\partial t} + (\mathbf{u}^f + \mathbf{u}^p) \cdot \nabla \theta = -\mathcal{R} f(z)(w^f + w^p) - Pe \frac{\partial \theta}{\partial z} + \Delta \theta, \end{cases} \quad (6)$$

where

$$f(z) = \frac{Pe e^{Pe z}}{1 - e^{Pe}}$$

is the dimensionless basic temperature gradient.

**Remark 1** Due to the specific non-dimensionalization we used, as  $Pe \rightarrow 0$  (which is equivalent to consider the conduction solution in a bi-disperse layer), all singularities are removable, allowing (6) to tend to the standard system where no throughflow is present (see [8]). This follows as, utilizing De L'Hospital's rule, one gets

$$\lim_{Pe \rightarrow 0} f(z) = -1.$$

The initial conditions and the boundary conditions appended to system (6) are

$$\mathbf{u}^s(\mathbf{x}, 0) = \mathbf{u}_0^s(\mathbf{x}), \quad \pi^s(\mathbf{x}, 0) = \pi_0^s(\mathbf{x}), \quad \theta(\mathbf{x}, 0) = \theta_0(\mathbf{x}),$$

with  $\nabla \cdot \mathbf{u}_0^s = 0$ , for  $s = \{f, p\}$ , and

$$w^f = w^p = \theta = 0 \quad \text{on } z = 0, 1, \quad (7)$$

respectively. According to experimental results, we will assume that  $\mathbf{u}^s, \theta \in W^{1,2}(V)$ ,  $\forall t \in \mathbb{R}^+$ , with  $s = \{f, p\}$ , are periodic functions in the  $(x, y)$  directions of period  $2\pi/l$  and  $2\pi/m$ ,  $V = \left[0, \frac{2\pi}{l}\right] \times \left[0, \frac{2\pi}{m}\right] \times [0, 1]$  being the periodicity cell.

Let us consider the third components of the double curl of the momentum equations (6)<sub>1</sub> and (6)<sub>2</sub>, hence the linear and the nonlinear stability analyses of the throughflow solution will be performed on the following system

$$\begin{cases} (1 + \gamma_1) \Delta w^f - \Delta w^p - \mathcal{R} \Delta_1 \theta = 0, \\ -\Delta w^f + (1 + \gamma_2) \Delta w^p - \mathcal{R} \Delta_1 \theta = 0, \\ \nabla \cdot \mathbf{u}^f = 0, \\ \nabla \cdot \mathbf{u}^p = 0, \\ \frac{\partial \theta}{\partial t} + (\mathbf{u}^f + \mathbf{u}^p) \cdot \nabla \theta = -\mathcal{R} f(z)(w^f + w^p) - Pe \frac{\partial \theta}{\partial z} + \Delta \theta, \end{cases} \quad (8)$$

where  $\Delta_1 = \partial^2/\partial x^2 + \partial^2/\partial y^2$  is the horizontal Laplacian.

### 3 Linear instability analysis

Since system (6) is autonomous, let us seek for perturbed solutions with exponential time dependence (i.e.  $e^{\sigma t}$ ,  $\sigma \in \mathbb{C}$  being the growth rate of the system) in the linearised perturbations system. Therefore, the linear instability threshold is to recover from the analysis of the linearised version of system (8), i.e.

$$\begin{cases} (1 + \gamma_1)\Delta w^f - \Delta w^p - \mathcal{R}\Delta_1\theta = 0, \\ -\Delta w^f + (1 + \gamma_2)\Delta w^p - \mathcal{R}\Delta_1\theta = 0, \\ \sigma\theta = -\mathcal{R}f(z)(w^f + w^p) - Pe\frac{\partial\theta}{\partial z} + \Delta\theta, \end{cases} \tag{9}$$

under the boundary conditions  $w^f = w^p = \theta = 0$  on  $z = 0, 1$ . System (9) is equivalent to

$$\begin{cases} \Delta w^f = \frac{2 + \gamma_2}{\gamma_1 + \gamma_2 + \gamma_1\gamma_2}\mathcal{R}\Delta_1\theta, \\ \Delta w^p = \frac{2 + \gamma_1}{\gamma_1 + \gamma_2 + \gamma_1\gamma_2}\mathcal{R}\Delta_1\theta, \\ \sigma\theta = -\mathcal{R}f(z)(w^f + w^p) - Pe\frac{\partial\theta}{\partial z} + \Delta\theta. \end{cases} \tag{10}$$

Let us denote by  $\langle \cdot, \cdot \rangle$ ,  $\| \cdot \|$  and  $*$ , inner product and norm on the Hilbert space  $L^2(V)$  and the complex conjugate of a field, respectively.

**Theorem 1** *The principle of exchange of stabilities holds for system (7)–(10), therefore convective instabilities can arise only through steady motions.*

**Proof** Let us employ the following transformation

$$\theta = e^{\frac{Pe}{2}z}\Phi \tag{11}$$

in system (10), which becomes

$$\begin{cases} \Delta w^f = \mathcal{R}c_1e^{\frac{Pe}{2}z}\Delta_1\Phi, \\ \Delta w^p = \mathcal{R}c_2e^{\frac{Pe}{2}z}\Delta_1\Phi, \\ \sigma e^{\frac{Pe}{2}z}\Phi = -\mathcal{R}f(z)(w^f + w^p) - \frac{Pe^2}{4}e^{\frac{Pe}{2}z}\Phi + e^{\frac{Pe}{2}z}\Delta\Phi, \end{cases} \tag{12}$$

where we set  $c_1 = \frac{2 + \gamma_2}{\gamma_1 + \gamma_2 + \gamma_1\gamma_2}$  and  $c_2 = \frac{2 + \gamma_1}{\gamma_1 + \gamma_2 + \gamma_1\gamma_2}$ . Employing the periodicity of the perturbation fields in the horizontal directions  $x$  and  $y$  and according to the

boundary conditions (7), we can assume the solutions be two-dimensional periodic waves of assigned wavenumber:

$$\phi(x, y, z) = \bar{\phi}(z)e^{i(lx+my)} \quad \forall \phi \in \{w^f, w^p, \Phi\}. \quad (13)$$

Since  $f(z) = \frac{Pe e^{Pe z}}{1 - e^{Pe}}$ , by virtue of (13), we get

$$\begin{cases} (D^2 - a^2)\bar{w}^f = -c_1 \mathcal{R} a^2 e^{\frac{Pe}{2}z} \bar{\Phi}, \\ (D^2 - a^2)\bar{w}^p = -c_2 \mathcal{R} a^2 e^{\frac{Pe}{2}z} \bar{\Phi}, \\ \sigma e^{\frac{Pe}{2}z} \bar{\Phi} = -\mathcal{R} \frac{Pe}{1 - e^{Pe}} e^{Pe z} (\bar{w}^f + \bar{w}^p) - \frac{Pe^2}{4} e^{\frac{Pe}{2}z} \bar{\Phi} + e^{\frac{Pe}{2}z} (D^2 - a^2) \bar{\Phi}, \end{cases} \quad (14)$$

where  $D = \frac{d}{dz}$ , while  $a^2 = l^2 + m^2$  is the overall wavenumber. Multiplying (14)<sub>3</sub> by  $e^{-\frac{Pe}{2}z}$ , we get

$$\sigma \bar{\Phi} = -\mathcal{R} \frac{Pe}{1 - e^{Pe}} e^{\frac{Pe}{2}z} (\bar{w}^f + \bar{w}^p) - \frac{Pe^2}{4} \bar{\Phi} + (D^2 - a^2) \bar{\Phi}. \quad (15)$$

Let us multiply (14)<sub>1</sub> by  $\bar{w}^{f*}$ , (14)<sub>2</sub> by  $\bar{w}^{p*}$ , (15) by  $\bar{\Phi}^*$  and let us integrate the resulting equations over  $[0, 1]$ , hence we obtain

$$\begin{aligned} \frac{1}{c_1} \left( \|D\bar{w}^f\|_{L^2(0,1)}^2 + a^2 \|\bar{w}^f\|_{L^2(0,1)}^2 \right) &= \mathcal{R} a^2 \int_0^1 e^{\frac{Pe}{2}z} \bar{\Phi} \bar{w}^{f*} dz, \\ \frac{1}{c_2} \left( \|D\bar{w}^p\|_{L^2(0,1)}^2 + a^2 \|\bar{w}^p\|_{L^2(0,1)}^2 \right) &= \mathcal{R} a^2 \int_0^1 e^{\frac{Pe}{2}z} \bar{\Phi} \bar{w}^{p*} dz, \\ \sigma \|\bar{\Phi}\|_{L^2(0,1)}^2 &= -\mathcal{R} \frac{Pe}{1 - e^{Pe}} \int_0^1 e^{\frac{Pe}{2}z} \bar{\Phi}^* (\bar{w}^f + \bar{w}^p) dz \\ &\quad - \frac{Pe^2}{4} \|\bar{\Phi}\|_{L^2(0,1)}^2 \\ &\quad - (\|D\bar{\Phi}\|_{L^2(0,1)}^2 + a^2 \|\bar{\Phi}\|_{L^2(0,1)}^2). \end{aligned} \quad (16)$$

By virtue of (16)<sub>1,2</sub> one has that  $\int_0^1 e^{\frac{Pe}{2}z} \bar{\Phi}^* (\bar{w}^f + \bar{w}^p) dz \in \mathbb{R}$ , therefore from (16)<sub>3</sub> it follows  $Im(\sigma) \|\bar{\Phi}\|_{L^2(0,1)}^2 = 0 \Rightarrow Im(\sigma) = 0$ , i.e.  $\sigma \in \mathbb{R}$ .  $\square$

Let us assume  $\sigma = 0$  in (10). Using solutions (13) in system (10), one obtains

$$\begin{cases} D^2 \bar{w}^f = a^2 \bar{w}^f - c_1 \mathcal{R} a^2 \bar{\theta}, \\ D^2 \bar{w}^p = a^2 \bar{w}^p - c_2 \mathcal{R} a^2 \bar{\theta}, \\ D^2 \bar{\theta} = a^2 \bar{\theta} + Pe D \bar{\theta} + \mathcal{R} f(z) (\bar{w}^f + \bar{w}^p). \end{cases} \quad (17)$$

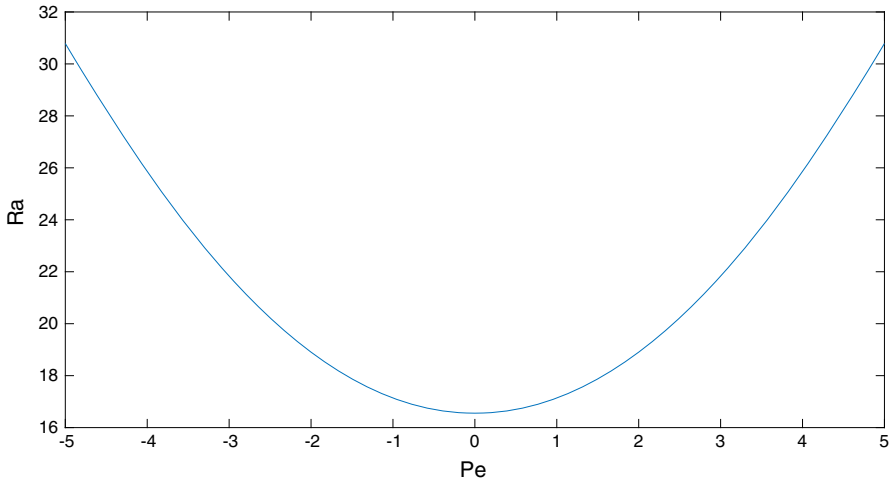


Fig. 1  $\gamma_1 = 2, \gamma_2 = 0.2$ . Stationary instability threshold as function of the Peclet number  $Pe$

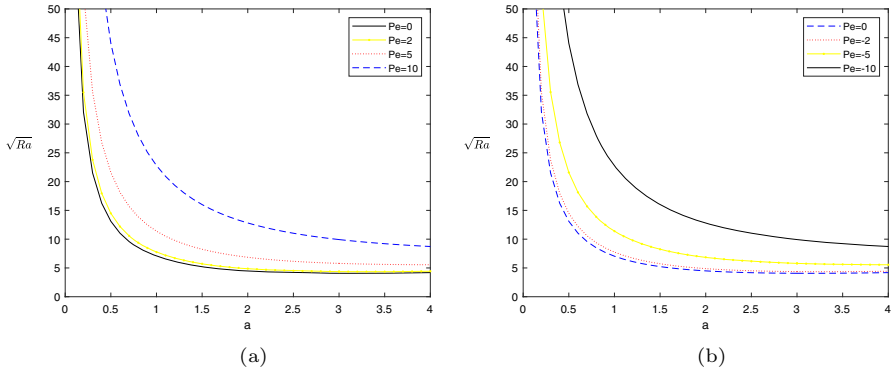


Fig. 2  $\gamma_1 = 2, \gamma_2 = 0.2$  **a** Stationary instability thresholds for positive quoted values of the Peclet number  $Pe$ . **b** Stationary instability thresholds for negative quoted values of the Peclet number  $Pe$

In order to find the instability threshold for the onset of *steady* convective instabilities, that is

$$\mathcal{R}_L = \min_{a^2 \in \mathbb{R}^+} \{ \mathcal{R}^2(a^2) | \mathcal{R}^2 \text{ verifies (17)} \},$$

system (17) needs to be solved. Let us underline that (7)–(17) is a boundary value problem of second order ODEs in the variable  $z$  and it has been numerically solved via MatLab software, employing a user-written code based on a combination of the Shooting Method and the Newton–Raphson Method.

The overall behaviour of the steady instability threshold as function of the Peclet number is shown in Fig. 1. Solving the boundary value problem (7)–(17) for quoted values of the Peclet number, we obtain the thresholds depicted in Fig. 2: in Fig. 2a the thresholds are plotted for  $Pe > 0$  and it is shown the *stabilizing effect* of a vertical



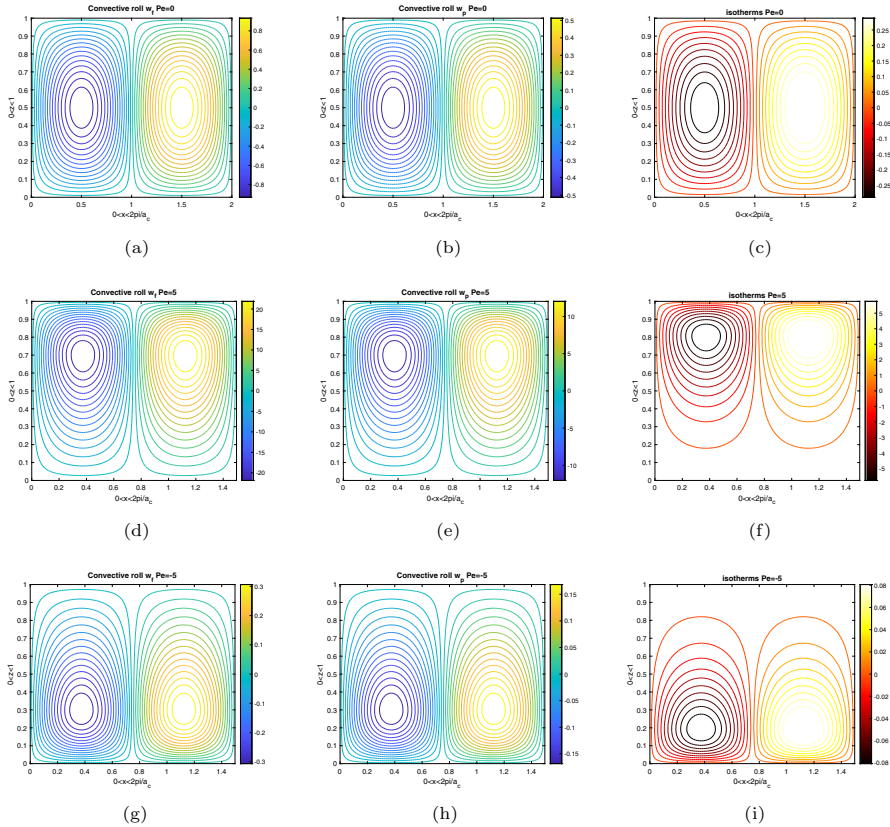


Fig. 3  $\gamma_1 = 2, \gamma_2 = 0.2$  Convective rolls and isotherms for quoted value of the Pelet number

constant upward throughflow on system dynamics, while the thresholds in Fig. 2b are depicted for  $Pe < 0$  and show that a vertical constant downward throughflow has a *destabilizing effect* on system dynamics.

Finally, in Fig. 3 the convective rolls and the isotherms are plotted for quoted value of the Pelet number. As  $|Pe|$  increases, the convective rolls lose the symmetry that characterizes the limit case  $Pe \rightarrow 0$ . In particular, for high positive Pelet numbers, we can observe a progressive detachment of the kinematic and temperature fields from the lower surface, hence the convective motion is confined near the surface toward which the throughflow is directed. Similarly, for high negative Pelet numbers, there is a detachment of the kinematic and temperature fields from the upper surface.

### 4 Nonlinear stability analysis

The aim of this Section is to analyse the stability of the throughflow solution (3) considering the full nonlinear system (8).

### 4.1 Differential constraint approach

In the present Section the differential constraint approach (see [14]) will be applied to system (8). Therefore, retaining (8)<sub>1,2</sub> as constraints, let us define

$$\begin{aligned} \hat{E} &= \frac{1}{2} \|\theta\|^2, \\ \hat{I} &= - \langle f(z)(w^f + w^p), \theta \rangle, \quad \hat{D} = \|\nabla\theta\|^2, \end{aligned} \tag{18}$$

therefore, multiplying (8)<sub>5</sub> by  $\theta$  and integrating over the periodicity cell  $V$ , we get

$$\frac{d\hat{E}}{dt} = \mathcal{R}\hat{I} - \hat{D} \leq -\hat{D} \left(1 - \frac{\mathcal{R}}{\mathcal{R}_N}\right), \tag{19}$$

where

$$\frac{1}{\mathcal{R}_N} = \max_{\mathcal{H}^*} \frac{\hat{I}}{\hat{D}} \tag{20}$$

and

$$\begin{aligned} \mathcal{H}^* &= \{(w^f, w^p, \theta) \in (H^1)^3 \mid w^f = w^p = \theta = 0 \text{ on } z = 0, 1; \text{ periodic in } x, y \\ &\text{with periods } 2\pi/l, 2\pi/m; \hat{D} < \infty; \text{ verifying (8)}_{1,2}\}. \end{aligned}$$

**Remark 2** Let us observe that the boundedness of  $\frac{\hat{I}}{\hat{D}}$  in  $\mathcal{H}^*$  is guaranteed by (8)<sub>1</sub> and (8)<sub>2</sub>. In fact, multiplying (8)<sub>1</sub> and (8)<sub>2</sub> by  $w^f$  and  $w^p$ , respectively, integrating over the periodicity cell and adding the resulting equations, we get

$$c_P \left( \gamma_1 \|w^f\|^2 + \gamma_2 \|w^p\|^2 \right) \leq \mathcal{R}^2 \left( \frac{1}{\gamma_1} + \frac{1}{\gamma_2} \right) \|\theta\|^2, \tag{21}$$

where the arithmetic–geometric mean, the Cauchy-Schwartz and the Poincaré inequalities were used, and where  $c_P(V)$  is the Poincaré constant. Accounting for the definitions of  $\hat{I}$  and  $\hat{D}$  and since  $f(z)$  is bounded in  $[0, 1]$ , by virtue of (21) it immediately follows that the ratio  $\frac{\hat{I}}{\hat{D}}$  is bounded in  $\mathcal{H}^*$ .

The variational problem (20) is actually equivalent to

$$\frac{1}{\mathcal{R}_N} = \max_{\mathcal{H}} \frac{\hat{I} + \int_V \lambda' f_1 dV + \int_V \lambda'' f_2 dV}{\hat{D}}, \tag{22}$$

where  $\lambda'(\mathbf{x})$  and  $\lambda''(\mathbf{x})$  are suitable Lagrange multipliers and

$$f_1 = (1 + \gamma_1)\Delta w^f - \Delta w^p - \mathcal{R}\Delta_1\theta, \quad f_2 = -\Delta w^f + (1 + \gamma_2)\Delta w^p - \mathcal{R}\Delta_1\theta,$$

$\mathcal{H} = \{(w^f, w^p, \theta) \in (H^1)^3 \mid w^f = w^p = \theta = 0 \text{ on } z = 0, 1; \text{ periodic in } x, y$   
with periods  $2\pi/l, 2\pi/m$ , respectively;  $\hat{D} < \infty\}$ .

**Theorem 2** *Condition  $\mathcal{R} < \mathcal{R}_N$  guarantees the global, nonlinear, asymptotic, exponential stability in the  $\hat{E}$ -norm of the throughflow solution (3).*

**Proof** Applying the Poincaré inequality one obtains that  $\hat{D} \geq \pi^2 \|\theta\|^2$ , hence from the energy equation (19) it follows that the condition  $\mathcal{R} < \mathcal{R}_N$  implies  $\hat{E}(t) \rightarrow 0$  at least exponentially. Moreover, multiplying the momentum equations (6)<sub>1</sub> and (6)<sub>2</sub> by the kinematic fields  $\mathbf{u}^f$  and  $\mathbf{u}^p$ , integrating over the periodicity cell and adding the resulting equations, by virtue of the arithmetic–geometric mean inequality and Cauchy–Schwartz inequality we get

$$\gamma_1 \|\mathbf{u}^f\|^2 + \gamma_2 \|\mathbf{u}^p\|^2 \leq \mathcal{R}^2 \left( \frac{1}{\gamma_1} + \frac{1}{\gamma_2} \right) \|\theta\|^2. \quad (23)$$

Therefore, by virtue of estimate (23), we can conclude that condition  $\mathcal{R} < \mathcal{R}_N$  guarantees the exponential stability of the throughflow solution with respect to the  $\hat{E}$ -norm.  $\square$

The Euler-Lagrange equations associated to the maximum problem (22) are

$$\begin{cases} (1 + \gamma_1)\Delta w^f - \Delta w^p - \mathcal{R}_N \Delta_1 \theta = 0, \\ -\Delta w^f + (1 + \gamma_2)\Delta w^p - \mathcal{R}_N \Delta_1 \theta = 0, \\ -\mathcal{R}_N f(z)(w^f + w^p) - \mathcal{R}_N^2 \Delta_1 (\lambda' + \lambda'') + 2\Delta \theta = 0, \\ -f(z)\theta + (1 + \gamma_1)\Delta \lambda' - \Delta \lambda'' = 0, \\ -f(z)\theta - \Delta \lambda' + (1 + \gamma_2)\Delta \lambda'' = 0. \end{cases} \quad (24)$$

Assuming solutions (13) in (24), we obtain

$$\begin{cases} D^2 \bar{w}^f = a^2 \bar{w}^f - c_1 \mathcal{R}_N a^2 \bar{\theta}, \\ D^2 \bar{w}^p = a^2 \bar{w}^p - c_2 \mathcal{R}_N a^2 \bar{\theta}, \\ D^2 \bar{\theta} = a^2 \bar{\theta} + \frac{\mathcal{R}_N}{2} f(z)(\bar{w}^f + \bar{w}^p) - \frac{\mathcal{R}_N^2}{2} a^2 (\bar{\lambda}' + \bar{\lambda}''), \\ D^2 \bar{\lambda}' = a^2 \bar{\lambda}' + c_1 f(z) \bar{\theta}, \\ D^2 \bar{\lambda}'' = a^2 \bar{\lambda}'' + c_2 f(z) \bar{\theta}. \end{cases} \quad (25)$$

The critical nonlinear threshold  $\mathcal{R}_N$  has been numerically found solving the boundary value problem (7)–(25), employing the same technique described in the previous Section. In the following numerical simulations, our results were tested for the dimensionless physical parameters  $\gamma_1 = 2$  and  $\gamma_2 = 0.2$  (see [15, 16]). In Fig. 4 the linear instability threshold  $\mathcal{R}_L$  and the nonlinear stability threshold with respect to  $\hat{E}$ -norm  $\mathcal{R}_N$  are depicted for quoted values of the Peclet number (for  $Pe \rightarrow 0$  in 4a and for

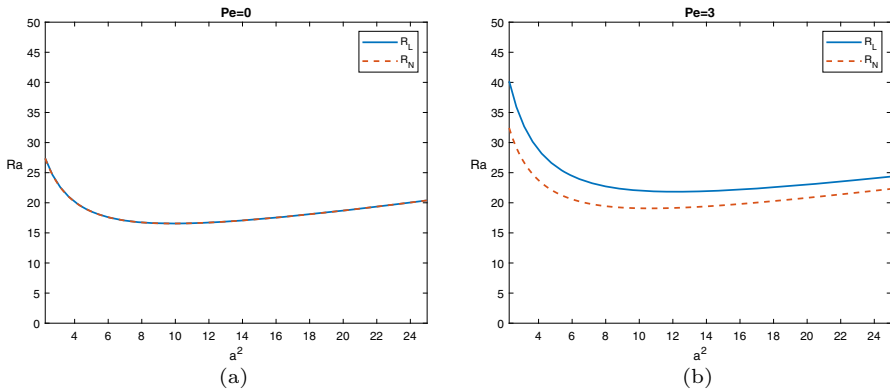


**Fig. 4** **a**  $\mathcal{R}_L$  and  $\mathcal{R}_N$  for  $Pe = 0$  and  $\gamma_1 = 2, \gamma_2 = 0.2$ . **b**  $\mathcal{R}_L$  and  $\mathcal{R}_N$  for  $Pe = 3$  and  $\gamma_1 = 2, \gamma_2 = 0.2$

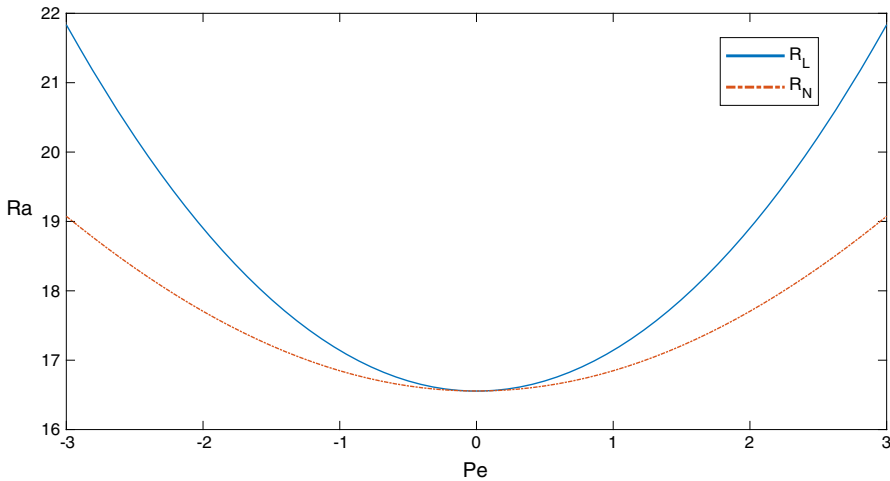


**Fig. 5** Linear instability threshold  $\mathcal{R}_L$ , nonlinear stability threshold  $\mathcal{R}_N$  as function of the Peclet number  $Pe$ , for  $\gamma_1 = 2, \gamma_2 = 0.2$

$Pe = 3$  in 4b). For  $Pe \rightarrow 0$  the coincidence between  $\mathcal{R}_L$  and  $\mathcal{R}_N$  is recovered, but as  $|Pe|$  increases, the gap between the linear threshold and the nonlinear threshold increases, as clearly depicted in Fig. 5, where the instability threshold  $\mathcal{R}_L$  and the nonlinear stability threshold  $\mathcal{R}_N$  are plotted as functions of the Peclet number  $Pe$ .

**Remark 3** In [8], the onset of convection for a single temperature bi-disperse porous medium was analysed, the instability threshold is:

$$\mathcal{R}_c = \min_{n, a^2} \frac{(n^2 \pi^2 + a^2)^2}{a^2} \frac{\gamma_1 \gamma_2 + \gamma_1 + \gamma_2}{\gamma_1 + \gamma_2 + 4}$$

Let us underline that if the throughflow is not considered (i.e.  $Pe \rightarrow 0$ ), we found  $\mathcal{R}_c = \mathcal{R}_L = \mathcal{R}_N = 16.5555$  (with  $\gamma_1 = 2, \gamma_2 = 0.2$ ), hence the stability results found in [8] are recovered.

## 4.2 Weighted energy method

In this Section, we will perform the nonlinear stability analysis applying the weighted energy method to the nonlinear boundary value problem (8)<sub>1</sub>, (8)<sub>2</sub>, (8)<sub>5</sub> in  $w^f, w^p, \theta$ , i.e.

$$\begin{cases} (1 + \gamma_1)\Delta w^f - \Delta w^p - \mathcal{R}\Delta_1\theta = 0, \\ -\Delta w^f + (1 + \gamma_2)\Delta w^p - \mathcal{R}\Delta_1\theta = 0, \\ \frac{\partial \theta}{\partial t} + (\mathbf{u}^f + \mathbf{u}^p) \cdot \nabla \theta = -\mathcal{R}f(z)(w^f + w^p) - Pe \frac{\partial \theta}{\partial z} + \Delta \theta, \\ w^f = w^p = \theta = 0 \quad \text{on } z = 0, 1. \end{cases} \quad (26)$$

The following result holds true.

**Theorem 3 (Weighted Poincaré Inequality)** *If  $\Phi \in \mathcal{H}$ , with*

$$\mathcal{H} = \{\phi \in H^1(V) \mid \phi = 0 \text{ on } z = 0, 1; \text{ periodic in } x, y \text{ with periods } 2\pi/l, 2\pi/m, \text{ respectively}\},$$

then

$$\langle e^{Pe z}, \Phi^2 \rangle \leq \frac{4}{4\pi^2 + Pe^2} \langle e^{Pe z}, |\nabla \Phi|^2 \rangle. \quad (27)$$

**Proof** Since  $\theta = e^{\frac{Pe}{2}z}\Phi$  is periodic on the  $x$  and  $y$  directions and vanishes on  $z = 0, 1$ , one gets (see [17–19])

$$\int_V \left( e^{\frac{Pe}{2}z} \Phi \right)^2 dV \leq \frac{1}{\pi^2} \int_V \left[ \frac{\partial}{\partial z} \left( e^{\frac{Pe}{2}z} \Phi \right) \right]^2 dV. \quad (28)$$

In view of the identity

$$\int_V \left[ \frac{\partial}{\partial z} \left( e^{\frac{Pe}{2}z} \Phi \right) \right]^2 dV = -\frac{Pe^2}{4} \int_V e^{Pe z} \Phi^2 dV + \int_V e^{Pe z} \left( \frac{\partial \Phi}{\partial z} \right)^2 dV, \quad (29)$$

from (28), it follows

$$\left( 1 + \frac{Pe^2}{4\pi^2} \right) \int_V e^{Pe z} \Phi^2 dV \leq \frac{1}{\pi^2} \int_V e^{Pe z} |\nabla \Phi|^2 dV, \quad (30)$$

therefore, one obtains (27).  $\square$

Now, considering the transformation (11), (26) becomes

$$\begin{cases} (1 + \gamma_1)\Delta w^f - \Delta w^p - \mathcal{R} e^{\frac{Pe}{2}z} \Delta_1 \Phi = 0, \\ -\Delta w^f + (1 + \gamma_2)\Delta w^p - \mathcal{R} e^{\frac{Pe}{2}z} \Delta_1 \Phi = 0, \\ e^{\frac{Pe}{2}z} \frac{\partial \Phi}{\partial t} + (\mathbf{u}^f + \mathbf{u}^p) \cdot \nabla \left( e^{\frac{Pe}{2}z} \Phi \right) = -\mathcal{R} f(z)(w^f + w^p) - \frac{Pe^2}{4} e^{\frac{Pe}{2}z} \Phi + e^{\frac{Pe}{2}z} \Delta \Phi, \\ w^f = w^p = \Phi = 0 \quad \text{on } z = 0, 1. \end{cases} \tag{31}$$

Let us multiply (31)<sub>1</sub> by  $w^f$ , (31)<sub>2</sub> by  $w^p$  and (31)<sub>3</sub> by  $e^{\frac{Pe}{2}z} \Phi$ , integrating each equation over the periodicity cell  $V$  and adding the resulting equations one obtains

$$\frac{d\mathcal{E}}{dt} = \mathcal{R}\mathcal{I} - \mathcal{D} + \frac{Pe^2}{2}\mathcal{E}, \tag{32}$$

where

$$\begin{aligned} \mathcal{E} &= \frac{\mu}{2} \left\langle e^{Pe^z}, \Phi^2 \right\rangle, \\ \mathcal{I} &= - \left\langle e^{\frac{Pe}{2}z} \Delta_1 \Phi, w^f + w^p \right\rangle - \mu \left\langle e^{\frac{Pe}{2}z} f(z) \Phi, w^f + w^p \right\rangle, \\ \mathcal{D} &= \gamma_1 \|\nabla w^f\|^2 + \gamma_2 \|\nabla w^p\|^2 + \|\nabla w^f - \nabla w^p\|^2 + \mu \left\langle e^{Pe^z}, |\nabla \Phi|^2 \right\rangle, \end{aligned} \tag{33}$$

and  $\mu$  a positive coupling parameter to be suitably chosen later. Setting

$$\frac{1}{\mathcal{R}_W} = \max_{\mathcal{H}} \frac{\mathcal{I}}{\mathcal{D}}, \tag{34}$$

the following theorem holds.

**Theorem 4** *Let us set*

$$\mathcal{E}_1 = e^{-\frac{Pe^2}{2}t} \mathcal{E}, \tag{35}$$

*then the condition*

$$\mathcal{R} < \mathcal{R}_W \tag{36}$$

*guarantees the global, nonlinear, asymptotic, exponential stability of the throughflow solution (3) with respect to the  $\mathcal{E}_1$ -norm.*

**Proof** By virtue of (35), from (32) one obtains

$$\frac{d\mathcal{E}_1}{dt} = \mathcal{D} \left( \mathcal{R} \frac{\mathcal{I}}{\mathcal{D}} - 1 \right) e^{-\frac{Pe^2}{2}t}, \tag{37}$$

where by virtue of (27)

$$\mathcal{D} \geq \frac{4\pi^2 + Pe^2}{2} \mathcal{E}. \quad (38)$$

Moreover, accounting for (34) and (36), from (37) it follows that

$$\frac{d\mathcal{E}_1}{dt} \leq \frac{4\pi^2 + Pe^2}{2} \left( \frac{\mathcal{R}}{\mathcal{R}_W} - 1 \right) \mathcal{E}_1, \quad (39)$$

hence, integrating with respect to time  $t$ , one gets

$$\mathcal{E}_1(t) \leq \mathcal{E}_1(0) \exp \left[ \frac{(4\pi^2 + Pe^2)(R - R_W)}{2R_W} t \right], \quad \forall t \geq 0 \quad (40)$$

and hence the global, nonlinear, asymptotic, exponential stability of the throughflow solution (3) with respect to the  $\mathcal{E}_1$ -norm is obtained.  $\square$

**Remark 4** Let us underline that in the limit case  $Pe \rightarrow 0$ , from (35) we get that  $\mathcal{E}_1 = \mathcal{E}$  coincides with  $\hat{\mathcal{E}}$  defined in (18) choosing  $\mu = 1$ . Therefore, in the limit case for vanishing throughflow, one has to refer to the stability results obtained in [8] (as stated in Remark 3).

The Euler-Lagrange equations associated to the maximum problem (34), assuming solutions (13), are:

$$\begin{cases} D^2 \bar{w}^f = a^2 \bar{w}^f + \frac{c_1}{2} \mathcal{R}_W e^{\frac{Pe}{2}z} [\mu f(z) - a^2] \bar{\Phi}, \\ D^2 \bar{w}^p = a^2 \bar{w}^p + \frac{c_2}{2} \mathcal{R}_W e^{\frac{Pe}{2}z} [\mu f(z) - a^2] \bar{\Phi}, \\ D^2 \bar{\Phi} = a^2 \bar{\Phi} - Pe D \bar{\Phi} + \frac{1}{2\mu} e^{-\frac{Pe}{2}z} \mathcal{R}_W [\mu f(z) - a^2] (\bar{w}^f + \bar{w}^p). \end{cases} \quad (41)$$

We numerically solved (41) under the boundary conditions  $\bar{w}^f = \bar{w}^p = \bar{\Phi} = 0$  on  $z = 0, 1$ , in order to determine the critical threshold

$$\mathcal{R}_W = \max_{\mu} \min_{a^2} \{ \mathcal{R}^2(a^2, \mu) | \mathcal{R}^2 \text{ verifies (41)} \}.$$

In Fig. 6 all the stability thresholds we found are depicted as functions of the Peclet number  $Pe$ . From Fig. 6 we found that, while for  $Pe \rightarrow 0$  the coincidence between the thresholds is recovered, for increasing Peclet numbers the weighted energy method significantly reduces the region of subcritical instabilities.

## 5 Conclusions

In this paper the effect of a vertical constant steady net mass flow (throughflow) on the onset of convective instabilities is analysed in a horizontal layer of fluid-saturated

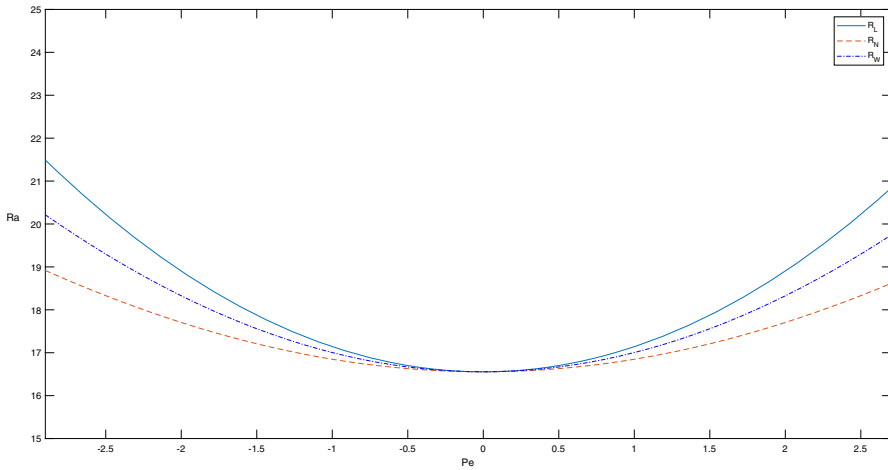


**Fig. 6** Linear instability threshold  $\mathcal{R}_L$ , nonlinear stability thresholds  $\mathcal{R}_N$  and  $R_W$  as function of the Peclet number  $Pe$ , for  $\gamma_1 = 2$ ,  $\gamma_2 = 0.2$

bi-disperse porous medium heated from below. We proved the validity of the principle of exchange of stabilities, therefore convective instabilities can arise only via steady motions. Via linear instability analysis of the throughflow solution, we determined the critical Rayleigh number for the onset of stationary convective instabilities and studied the behaviour of the critical Rayleigh number with respect to the Peclet number, proving that the throughflow has a stabilizing effect on the onset of convective instabilities when  $Pe > 0$ , destabilizing when  $Pe < 0$ . By mean of the differential constraints approach and the weighted energy method, we performed the nonlinear stability analysis of the throughflow solution, in order to catch the method that better describes the physics of the problem. We found that there is not coincidence between the linear and the nonlinear thresholds, therefore a region of subcritical instabilities is present, but, for increasing Peclet numbers, the thickness of the region of subcritical instabilities is significantly reduced by the weighted energy method.

**Acknowledgements** This paper has been performed under the auspices of the GNFM of INdAM.

**Author Contributions** All authors contributed to the study conception and design. Material preparation, data collection and analysis were performed by FC, RDeL and GM. All authors read and approved the final manuscript.

**Funding** Open access funding provided by Università degli Studi di Napoli Federico II within the CRUI-CARE Agreement. No funding was received to assist with the preparation of this manuscript.

**Availability of data and materials** Data sharing not applicable.

**Code Availability** Not applicable.



## Declarations

**Conflict of interest** The authors have no competing interests to declare that are relevant to the content of this article.

**Ethics approval** Not applicable.

**Consent to participate** Not applicable.

**Consent for publication** Not applicable.

**Open Access** This article is licensed under a Creative Commons Attribution 4.0 International License, which permits use, sharing, adaptation, distribution and reproduction in any medium or format, as long as you give appropriate credit to the original author(s) and the source, provide a link to the Creative Commons licence, and indicate if changes were made. The images or other third party material in this article are included in the article's Creative Commons licence, unless indicated otherwise in a credit line to the material. If material is not included in the article's Creative Commons licence and your intended use is not permitted by statutory regulation or exceeds the permitted use, you will need to obtain permission directly from the copyright holder. To view a copy of this licence, visit <http://creativecommons.org/licenses/by/4.0/>.

## References

1. Nield, D.A., Kuznetsov, A.V.: A two-velocity temperature model for a bi-dispersed porous medium: forced convection in a channel. *Trans. Porous Media* **59**, 325–339 (2005)
2. Nield, D.A., Kuznetsov, A.V.: Heat transfer in bidisperse porous media. *Transport Phenomena in Porous Media III*, 34–59 (2005)
3. Nield, D.A., Kuznetsov, A.V.: The onset of convection in a bidisperse porous medium. *Int. J. Heat Mass Transf.* **49**(17–18), 3068–3074 (2006)
4. Gentile, M., Straughan, B.: Bidispersive thermal convection with relatively large macropores. *J. Fluid Mech.* **898**, A14 (2020)
5. Badday, A.J., Harfash, A.J.: Chemical reaction effect on convection in bidispersive porous medium. *Transp. Porous Med.* **137**, 381–397 (2020)
6. Capone, F., De Luca, R., Fiorentino, L., Massa, G.: Bi-disperse convection under the action of an internal heat source. *Int. J. Non-Linear Mech.* **150**, 104360 (2023)
7. Imani, G., Hooman, K.: Lattice Boltzmann pore scale simulation of natural convection in a differentially heated enclosure filled with a detached or attached bidisperse porous medium. *Trans. Porous Media* **116**, 91–113 (2017)
8. Gentile, M., Straughan, B.: Bidispersive thermal convection. *Int. J. Heat Mass Transfer* **114**, 837–840 (2017)
9. Sutton, F.M.: Onset of convection in a porous channel with net through flow. *Phys. Fluids* **13**(8), 1931–1934 (1970)
10. Petrolo, D., Chiapponi, L., Longo, S., Celli, M., Barletta, A., Di Federico, V.: Onset of Darcy-Bénard convection under throughflow of a shear-thinning fluid. *J. Fluid Mech.* **889**, 2 (2020)
11. Capone, F., Gianfrani, J.A., Massa, G., Rees, D.A.S.: A weakly nonlinear analysis of the effect of vertical throughflow on Darcy-Bénard convection. *Phys. Fluids* **35**(1), 014107 (2023)
12. Gouin, H., Muracchini, A., Ruggeri, T.: On Muller paradox for thermal-incompressible media. *Continuum Mech. Thermodyn.* **24**, 505–513 (2011)
13. Falsaperla, P., Mulone, G., Straughan, B.: Bidispersive-inclined convection. *Proc. R. Soc. A* **472**(2192), 20160480 (2016)
14. Hill, A.A.: A differential constraint approach to obtain global stability for radiation-induced double-diffusive convection in a porous medium. *Math. Meth. Appl. Sci.* **32**(8), 914–921 (2009)
15. Capone, F., Gentile, M., Massa, G.: The onset of thermal convection in anisotropic and rotating bidisperse porous media. *Z. Angew. Math. Phys.* **72**, 169 (2021)
16. Gentile, M., Straughan, B.: Anisotropic bidispersive convection. *Proc. R. Soc. A.* **475**, 20190206 (2019)

17. Flavin, J.N., Rionero, S.: *Qualitative Estimates for Partial Differential Equations: An Introduction*. CRC Press, Boca Raton (1995)
18. Galdi, G.P., Rionero, S.: *Weighted energy methods in fluid dynamics and elasticity*. *Lecture Notes in Mathematics* (Springer) **1134** (1985)
19. Hill, A.A., Rionero, S., Straughan, B.: Global stability for penetrative convection with throughflow in a porous material. *IMA J. Appl. Math.* **72**(5), 635–643 (2007)

**Publisher's Note** Springer Nature remains neutral with regard to jurisdictional claims in published maps and institutional affiliations.